JOURNAL OF MOLECULAR SPECTROSCOPY **33**, 505–519 (1970)

Electronic Spectra and Structure of the Hydrogen Halides

The $b\ ^3\Pi_i$ and $C\ ^1\Pi$ States of HCl and DCl

S. G. TILFORD

E. O. Hulburt Center for Space Research, U. S. Naval Research Laboratory, Washington, D. C. 20390

M. L. GINTER[1] AND JOSEPH T. VANDERSLICE[1]

Institute for Molecular Physics, University of Maryland, College Park, Maryland 20740

The absorption spectra of the C–X and "B"–X transitions of HCl and DCl, which occur in the vacuum ultraviolet below 1350 Å, have been photographed at high resolution. Analyses show that the "B" state is a $^3\Pi_i$ (case a) state, designated here as $b\ ^3\Pi_i$, while the C state is $^1\Pi$. Both $b\ ^3\Pi_i$ and $C\ ^1\Pi$ originate from the same $\pi^3\sigma$ configuration and both states exhibit strong predissociations. Effective molecular constants are presented for the b and C states of the isotopic species $H^{35}Cl$, $D^{35}Cl$, and $D^{37}Cl$.

INTRODUCTION

The importance of the electronic spectrum and structure of the HCl molecule has increased sharply in recent years. As a constituent in planetary atmospheres (*1*), HCl may be of considerable astrophysical importance. As a molecular species with a $^2\Pi$ (case a) core, HCl can provide the first reliable data on molecular Rydberg states with non-Σ-type cores. Hence, it is somewhat surprising that relatively little experimental data exist for the excited electronic states of this molecule. In fact, one finds that the structures of the excited electronic states of the hydrogen halide molecules are among the most poorly understood of any diatomic molecule. The present paper is the first in a series in which extensive spectral data on the excited states of the hydrogen halides will be presented.

The known electronic spectra of HCl consist of (a) absorption and emission continua with maxima near ~1550 and 2570 Å, respectively (*2*, *3*); (b) discrete emission spectra in the 1800–2500 Å region (*3*); and (c) absorption bands extending from 1340 Å to above the first ionization limit (*4*). The continuous absorption spectrum in the ultraviolet has been assigned to transitions between the $X^1\Sigma^+$ state and the repulsive Π states (*5*) (often referred to as A or Q) which are cor-

[1] Partially supported by the E. O. Hulburt Center for Space Research.

related with the ground state atomic term limit. The discrete emission spectrum in the ultraviolet has been assigned to transitions between high vibrational levels of $X^1\Sigma^+$ and another $^1\Sigma^+$ state (generally referred to as $V^1\Sigma^+$) which has a large admixture of ion-pair states (*3*) while the continuous emission has been assigned (*3*) to the $V \rightarrow A$ transition. The absorption spectrum below 1340 Å was first studied at low dispersion by Price (*4*) who assigned several features to electronic states which he labeled B, B', C, and C'. From general considerations and Price's data, Mulliken (*5*) postulated that the B and C states were most likely a $^3\Pi_i$ and a $^1\Pi$ state, respectively, both states originating from the same $\pi^3\sigma$ configuration. Mulliken also concluded that the B' and C' bands ("satellite bands") should probably be associated with an additional $\pi^3\sigma$ configuration. Recently, the first members of the "B"–X and C–X transitions in DCl were observed under high dispersion by Stamper (*6*), who assigned both upper states as definitely Π-type. Finally, Nesbet (*7*) has performed Hartree-Fock MO calculations for the $X^1\Sigma^+$, $A^1\Pi$, $a^3\Pi$, $t^3\Sigma^+$, and $V^1\Sigma^+$ states,[2] and several general discussions exist (*8*) which are pertinent to the electronic structure of HCl.

In the present work high resolution spectral data were utilized in the characterization of the "B" and C states of HCl and DCl. In addition, it proved possible to assign these states unambiguously to a $^3\Pi_i$ and a $^1\Pi$ state, respectively, which originate from the same $\pi^3\sigma$ configuration. Transitions from the ground state to these two states account for *all* discrete absorption bands above 1240 Å, including the "B" and C progressions, the satellite progressions, and several previously unreported bands. The lowest lying configurations and corresponding electronic states for HCl can be summarized as follows:[2]

$\sigma^2\pi^4$	$X^1\Sigma^+$
$\sigma^2\pi^3\sigma^*$	$a^3\Pi$, $A^1\Pi$
$\sigma^2\pi^3\sigma$	$b^3\Pi_i$, $C^1\Pi$
$\sigma\pi^4\sigma^*$	$t^3\Sigma^+$, $V^1\Sigma^+$.

Of these, $X^1\Sigma^+$, $a^3\Pi$, $A^1\Pi$, and $t^3\Sigma^+$ are correlated with the ground state separated atom limit $^2P(\mathrm{Cl}) + {}^2S(\mathrm{H})$, a, A, and t being repulsive states.

EXPERIMENTAL METHODS

Absorption spectra of HCl and DCl were photographed in the region from 1070 to 1350 Å in the fourth and fifth orders of a 6.6-m focal-length vacuum spectrograph. Spectra also were obtained photoelectrically with a 1-m vacuum monochromator. The source of the background continuum was a windowless microwave

[2] In the older literature, X was sometimes referred to as N, a and A as Q, b as B, and t as T. For internuclear separations around r_e for the $X\ ^1\Sigma^+$ state, the $\sigma\pi^4\sigma^*$ configuration probably lies higher than the next $\pi^3\sigma$ and $\pi^3\pi$ (Rydberg) configurations which lie above the $\pi^3\sigma$ of b and C.

excited argon lamp (*9*). Exposure times ranged from 30 min to 4 hr. The sample gas was flowed through a 5-cm cell fitted with detachable lithium fluoride windows at pressures ranging from ~0.015 to 3 mm of Hg. During each exposure decomposition products formed a film on the windows which decreased the transmission of the cell to a few percent at the shorter wavelengths. Between exposures the cell was disassembled and the windows were polished to restore their original transmission. Spectroscopic grade HCl purchased from Matheson and DCl (99 at. % D) purchased from Isomet were used without further purification.

With DCl, considerable difficulty was experienced with isotopic exchange. Initial flushing of the system several times with D_2 together with the application of a Tesla discharge while the system was filled with D_2 reduced the amount of HCl present in subsequent DCl exposures to about 20–30%. Small amounts of uncontaminated DCl were produced by a dc-discharge in a cell, filled with deuterium gas, fitted with lithium fluoride windows attached with silver chloride.

The comparison spectra were second-order hollow-cathode iron lines (*10*). A least squares "line-search" computer program (*11*) was employed in the wavelength reduction. With this program, for a given plate, it is necessary to identify only two iron comparison lines in order to reduce all measured plate positions to final wavenumbers. For some plates it was necessary to apply a "plate racking" correction (*12*). With some few exceptions individual spectral lines were measured from 2 to 12 times on several different exposures, and the reported frequencies

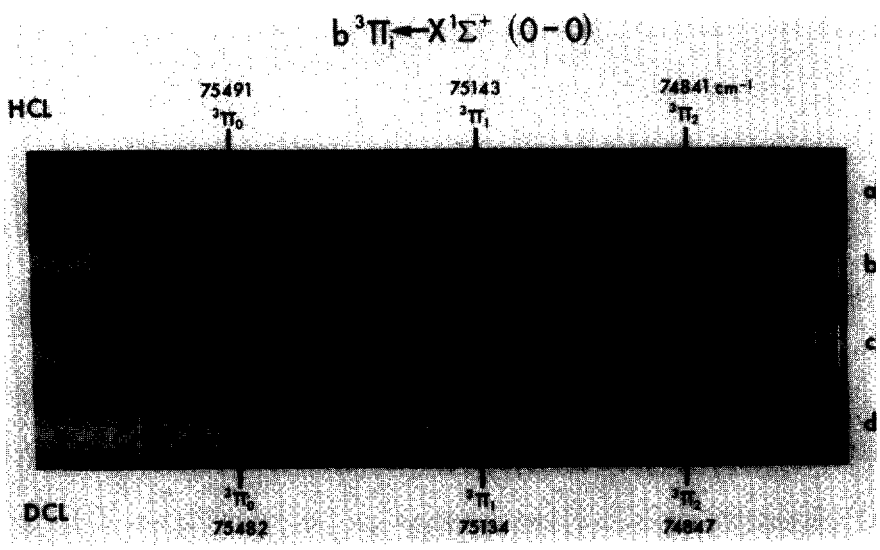

FIG. 1. The (0–0) bands of the $b\ ^3\Pi_i \leftarrow X\ ^1\Sigma^+$ transitions of HCl and DCl: spectra (a) and (b) are HCl, and spectra (c) and (d) are DCl with some HCl contamination. The origins of the three subbands of $b \leftarrow X$ are labeled by their appropriate upper state components $^3\Pi_0$, $^3\Pi_1$, and $^3\Pi_2$. A CO impurity band partially overlaps the $^3\Pi_0 \leftarrow X$ subband.

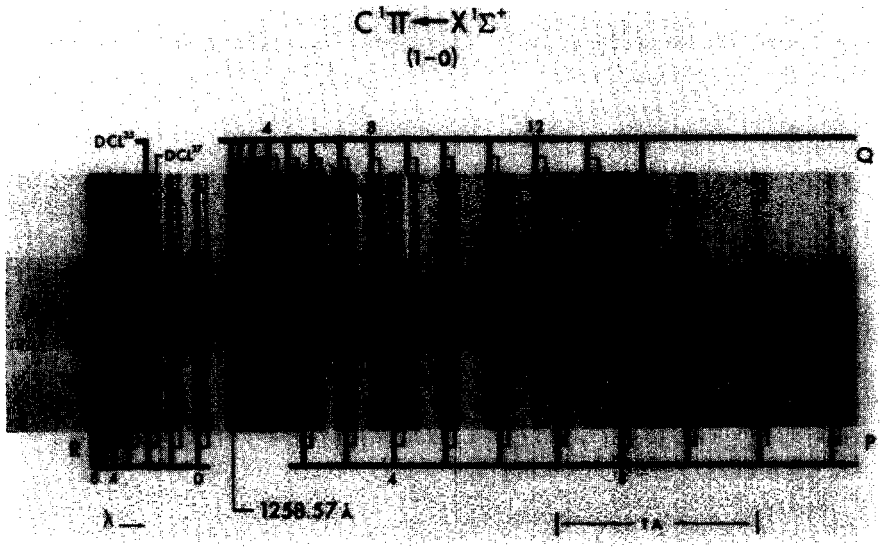

FIG. 2. The (1–0) band of the $C\ ^1\Pi \leftarrow X\ ^1\Sigma^+$ transition of DCl. The $D^{35}Cl$, $D^{37}Cl$ isotopic splitting is indicated by heavy and light lead lines, respectively.

are averages of all measurements. It is estimated that the absolute wavelengths may be in error by 0.005 Å corresponding to 0.35 cm^{-1} at 1200 Å. The relative error of sharp unblended lines is approximately 0.001 Å corresponding to 0.07 cm^{-1} at 1200 Å. For broad, diffuse, or blended lines the relative error may be a few tenths of a wavenumber.

RESULTS

A. General

In both HCl and DCl the first absorption which exhibits rotational fine structure occurs in the region below 1340 Å (see Fig. 1). It is obvious from Fig. 1. that the structure in this region consists of three bands corresponding to $\Delta\Lambda > 0$ with the central band, $b^3\Pi_1$, (the "*B*" state referred to in the Introduction) being by far the most intense. In this region, the DCl structure is slightly broadened while the HCl structure is diffuse, which indicates the existence of a predissociation.

The next absorption, which occurs to slightly shorter wavelengths, consists of the first member of the intense $C \leftarrow X$ transition, together with weaker bands which are the second members of the upper state vibrational progression of $b \leftarrow X$. In several instances, these vibrational progressions can be extended by at least one additional member, but in all cases the bands are quite diffuse (the exception being the second member of the DCl $^3\Pi_1 \leftarrow X$ progression, which does exhibit diffuse rotational structure). Relatively long upper state vibrational progressions are observed for the $C^1\Pi \leftarrow X^1\Sigma^+$ transition of both HCl and DCl. For

TABLE I

WAVENUMBERS OF THE BANDS OF THE $b\ ^3\Pi_i \leftarrow X\ ^1\Sigma^+$ TRANSITION OF HCl[a]

J	$^3\Pi_2 - X(0\text{–}0)$[b]	$^3\Pi_1 - X(0\text{–}0)$[c]		$^3\Pi_0 - X(0\text{–}0)$[c]	
	$Q(J)$	$P(J)$	$R(J)$	P(J)	R(J)
0			75 161.4		
1			180.8		75 531.5
2		75 100.5	198.3	75 448.8*	551.8
3	74 824.9	076.9	214.5	426.8	572.4
4	815.5	052.5	229.1	405.2	591.2
5	802.2	027.0	242.6	385.4	610.4*
6	786.0	75 000.3	255.7	363.1	630.0
7	769.3	74 972.6	266.2	340.6	647.0
8	750.2	944.0	275.0	318.3	664.5
9		913.3			681.5

[a] All branches are diffuse with the degree of diffuseness increasing with increasing rotational energy. Bands too diffuse for rotational analysis are listed in Table V. An asterisk indicates a blended line.

[b] R-head observed at 74 917 ± 5 cm^{-1}. $P(5)$ = 74 710.7; $P(6)$ = 74 676.7 cm^{-1}.

[c] Q-branch unresolved.

TABLE II

WAVENUMBERS OF THE BANDS OF THE $C\ ^1\Pi \leftarrow X\ ^1\Sigma^+$ TRANSITION OF HCl[a]

J	(0–0) Band[b]			(1–0) Band[c]	
	$P(J)$	$Q(J)$	$R(J)$	P(J)	R(J)
0			77 503.94		80 187.4
1		77 482.89*	520.38		204.8
2	77 440.47	478.86	534.69	80 125.5	219.0
3	416.27	472.18	546.43	100.2	
4	388.58	463.34*	556.20	071.3	
5	359.93	452.29	563.20	041.3	
6	327.22	438.67	568.09	80 010.5	
7	293.22	422.86		79 976.0	
8	257.80	405.93*		938.2	
9	218.36	384.63*			
10	177.86				

[a] All branch lines are somewhat diffuse with the degree of diffuseness increasing with increasing rotational energy. Bands too diffuse for rotational analyses are listed in Table V. An asterisk indicates a blended line.

[b] A number of very diffuse lines corresponding to higher J levels have been observed but are not reported here.

[c] Branch lines for this transition are very diffuse and no $H^{35}Cl$–$H^{37}Cl$ splitting is resolved. The head of the unresolved Q-branch is at 80 170 ± 3 cm^{-1} and the R-head is observed at 80 252 ± 5 cm^{-1}.

TABLE III

Wavenumbers of the Bands of the b $^3\Pi_1 \leftarrow X\ ^1\Sigma^+$ Transition of DCl.[a]

	$^3\Pi_2$ - X (0-0)			$^3\Pi_1$ - X (0-0)[b]		
J	P(J)	Q(J)	R(J)	P(J)	Q(J)	R(J)
0						75144.30
1					75132.79	153.65
2		74844.24	74873.65	75112.27*	131.92	162.56
3	74811.73*	841.25	880.18	099.77*	130.22	171.40
4	797.92	837.16	886.06	087.42	127.69	179.01
5	783.20*	832.22	890.98	074.49	124.74	186.29
6	767.86	826.39	894.98	061.09	121.43	193.29
7	751.22	819.44	897.83	046.87	117.11	199.78
8	733.66	811.73*	900.22	031.85	112.27*	204.59
9	715.28	803.07	901.00	016.89	106.23	209.27
10	696.07	793.31		75000.97	099.77*	213.94
11	675.80	783.20*		74984.63	094.09	217.57
12	654.67	771.56		967.64		220.59
13	632.68	759.29		949.92		
14		746.31		932.17		
15				912.30		

	$^3\Pi_0$ - X (0-0)			$^3\Pi_1$ - X (1-0)[c]		
J	P(J)	Q(J)	R(J)	P(J)	Q(J)	R(J)
0						77100.59
1	75469.95*					110.11
2	459.45*		75512.29	77067.41*		118.07
3	448.81*		521.68	056.45	77086.60	125.56
4	436.87		530.63	043.11*	082.48	132.31
5	424.60		539.19	028.13	078.64	138.19
6	412.25	75474.88	547.42	77013.71	072.80	143.24
7	399.36	472.58	555.29	76998.05	067.41*	147.35
8	386.30	469.95*	562.77	981.89	060.52	150.26
9	372.83	466.78	569.90	964.34	052.92	
10	359.09	463.18	576.43	946.25	043.11*	
11	344.89	459.45*	582.85	927.23	034.91	
12	330.40	455.13	588.71	908.00	025.16	
13	315.66	450.28	593.68	887.44		
14	300.13	445.75	598.53	866.16		
15		439.93	603.32	844.22		
16			607.05	821.33		
17			610.35*			

[a] An asterisk indicates a blended line. Bands too diffuse for rotational analyses are listed in Table V.

[b] Previously analyzed in part by Stamper (*6*).

[c] All branch lines are somewhat diffuse, with the degree of diffuseness increasing with increasing rotational energy. The values quoted here correspond to $D^{35}Cl$, the $D^{37}Cl$ lines being partially resolved shoulders on the low frequency side of each line.

TABLE IV

Wavenumbers of the Bands of the $C\ ^1\Pi \leftarrow X\ ^1\Sigma^+$ Transition of DCl.[a]

(0 - 0) Band[b]

J	P(J)	Q(J)	R(J)
0			77507.57
1		77496.49	516.37
2		494.89	524.03
3	77463.34*	491.91	531.12
4	448.95	487.96	536.69
5	434.44	482.89*	541.87
6	418.28	477.77	545.98
7	402.02	471.03	548.84
8	384.78*	463.34*	551.65
9	366.10	454.76	
10		445.65	
11		435.43	
12		424.77	

(1 - 0) Band

J	P(J)		Q(J)		R(J)	
0					79465.66	62.63
1			79454.95	52.27*	473.93	70.93*
2	79433.56	30.23*	452.27*	48.72*	480.99*	78.09*
3	419.91*	17.52	448.72*	45.85	486.92	83.83*
4	405.63	02.76	443.83	40.95	491.50*	88.34*
5	389.62*	87.09*	437.56	34.75	494.80*	91.50*
6	372.94*	70.45	430.23*	27.53	497.10*	94.48*
7	354.80	52.14	421.62	19.91*	497.10*	94.48*
8	335.43	32.94	412.09	09.20	497.10*	94.48*
9	314.98	12.40	400.94	98.32	494.80*	
10	293.24	90.92	389.17	87.09*	491.50*	
11	270.36	68.41	375.42	72.94*	488.34*	
12	246.52	44.32	361.02	58.33	483.85*	
13	221.43	19.37	345.39	42.86	478.09*	
14	195.35	93.44	328.72	26.22	470.93*	
15	168.28	66.25			462.21*	
16	139.92	38.15			452.27*	
17	110.65					
18	080.48					

HCl the bands rapidly become diffuse, with the third member in the series exhibiting no resolved rotational structure. For DCl, however, the branch lines are relatively sharp and rotational analyses were performed on the first five members of the observed (v'–0) progressions of both $D^{35}Cl$ and $D^{37}Cl$. The observed ^{35}Cl, ^{37}Cl isotopic shifts (see Fig. 2) were used to confirm (see below) the upper state vibrational numbering for the $C^1\Pi$ state of DCl. Intensity considerations (see be-

TABLE IV (continued)

(2 - 0) Band

J	P(J)		Q(J)		R(J)	
0					81357.44	51.90
1			81346.55	40.97	365.45*	59.61
2	81325.79*	20.38*	343.59*	38.90*	371.34*	65.45*
3	311.51*	06.70*	338.90*	33.44*	376.17*	71.34*
4	295.49*	90.60*	333.44*	27.74	379.80	74.55*
5	279.39	74.19	325.79*	20.38*	381.54*	76.17*
6	261.31	56.07	317.27*	11.51*	381.54*	76.17*
7	241.71	36.56	306.70*	01.59*	381.54*	76.17*
8	220.66	15.58	295.49*	90.13*	378.53	74.55*
9	198.25	93.41	281.87	76.68	374.55*	68.75*
10	174.34	69.46	267.34	62.27	368.75*	
11	149.16	44.29	251.29	46.03	361.80	
12	122.24	17.70	233.57	28.66	353.00	
13	094.41	89.75	214.28*	09.93	343.59*	
14	065.01	60.28	194.28	90.39*		
15	034.10	29.55		67.72		
16	81002.00			44.86		
17	80968.62					

(3 - 0) Band

J	P(J)		Q(J)		R(J)	
0					83184.71*	77.34
1			83174.07	65.63*	192.32*	84.71*
2	83152.02	44.68*	170.75*	63.01	197.73	89.66*
3	138.69	31.22	165.63*	57.81	201.76	93.83
4	122.46	13.87*	158.61*	50.40*	203.97*	95.74*
5	105.00*	97.48	150.40*	42.39	203.97*	95.74*
6	085.75	78.18	139.93	32.14	203.97*	95.74*
7	064.45	56.31*	128.06	20.52	200.47	92.32*
8	041.95	34.60	113.87*	06.45	195.74*	87.24
9	83017.58	10.73*	099.12	91.75	189.66*	
10	82991.68		082.04	74.83	181.38	
11	964.01		063.61	56.31*	170.75*	
12	934.64		042.86		158.61*	
13	903.16		83020.81		144.68*	
14			82997.44			

low) and the observed HCl–DCl shifts served to identify the upper state vibrational numbering in the $C^1\Pi$ and $b^3\Pi_i$ states of HCl, and the $b^3\Pi_i$ state of DCl. Rotational analyses of the (0–0) bands of $b^3\Pi_i \leftarrow X^1\Sigma^+$ of HCl and DCl, the (1–0) band of $b^3\Pi_1 \leftarrow X^1\Sigma^+$ of DCl, the (1–0) and (0–0) bands of $C^1\Pi \leftarrow X^1\Sigma^+$ of HCl, and the (0–0), (1–0), (2–0), (3–0), and (4–0) bands of $C^1\Pi \leftarrow X^1\Sigma^+$ of DCl are presented in Tables I–IV. Additional data on bands too diffuse for rotational analyses appear in Table V. The observed vibrational levels of the b and C states for HCl and DCl are summarized in Fig. 3.

TABLE IV (continued)

	(4 - 0) Band					
J	P(J)		Q(J)		R(J)	
1			84939.13*	30.37*	84958.43*	47.96*
2			936.23	26.72*	962.80*	52.55*
3	84903.66*	93.49	930.37*	20.40*	965.93*	55.68*
4	887.52*	77.32*	922.28	12.81*	966.57	55.68*
5	868.28	58.79	912.81*	03.66*	965.93*	55.68*
6	848.33*	38.40	901.29*	91.51*	962.80*	52.55*
7	826.14*	16.21	887.52*	77.94*	958.43*	47.96*
8	801.86	91.73*	872.31	62.37	951.14*	41.75*
9	775.61*	66.32*	855.04	45.80	941.75*	32.54*
10	747.81	36.71*	835.83	26.14*	932.54*	23.62*
11	717.96	08.57	814.64*	04.99	920.40*	10.76
12	685.77		791.73*	81.38*	905.30	
13	652.52		766.32*	56.72*		
14	616.92					

a. When two numbers are listed for a branch line, the left hand number corresponds to DCl^{35} and the right hand member corresponds to DCl^{37}. An asterisk indicates a blended line.

b. Previously analysed in part by Stamper (6).

Approximate relative intensities for several bands of HCl were obtained photoelectrically, as well as photographically. The ratio of the (0–0) bands of $C^1\Pi \leftarrow X^1\Sigma^+$ to $b^3\Pi_1 \leftarrow X^1\Sigma^+$ is approximately 40–50:1. The intensities of the $b^3\Pi_0 \leftarrow X^1\Sigma^+$ and $b^3\Pi_2 \leftarrow X^1\Sigma^+$ transitions are approximately equal and about a factor of 50 weaker than the $b^3\Pi_1 \leftarrow X^1\Sigma^+$ transition. The (1–0) band of the C–X transition is approximately 8 times weaker than the (0–0) band, which is in agreement with the Franck-Condon principle since the upper state molecular constants are similar to those of the ground state. Within any given progression, relative intensities are very difficult to measure because of the rapid change in the degree of diffuseness from one vibrational level to the next. This is especially true in the $v' = 0$ and $v' = 1$ bands of the $b - X$ transition.

B. Molecular Constants

The rotational analyses of the bands were straightforward, since each band, when resolved, consisted of simple P-, Q-, and R-branches. Ground state data for $H^{35}Cl$, $D^{35}Cl$, and $D^{37}Cl$ were obtained from Rank *et al.* (*13*), Rank *et al.* (*14*), and Webb and Rao (*15*), respectively. These data are summarized in Table VI. For each molecule, assignments were checked with the appropriate ground state combination differences. Since the Λ-type doubling is small in the states under discussion ($q \leqq 0.015$ cm^{-1}, see below), the Q-branch lines could be assigned using

TABLE V

BAND ORIGINS AND EFFECTIVE ROTATIONAL CONSTANTS FOR THE $b\ ^3\Pi_i \leftarrow X\ ^1\Sigma^+$ AND $C\ ^1\Pi \leftarrow X\ ^1\Sigma^+$ TRANSITIONS IN HCl AND DCl[a]

Species	v'	ν_0	B_v	Comments
HCl				
$b\ ^3\Pi_2$	0	74 839.9	9.18	Diffuse structure; see Table I.
$b\ ^3\Pi_1$	0	75 142.6	9.87	Diffuse structure; see Table I.
$b\ ^3\Pi_0$	0	75 490.4	10.36	Diffuse structure; see Table I.
$b\ ^3\Pi_1$	1	(77 885 ± 15)[b]	(~9.3)[c]	Diffuse dbl. head; R − head = 77 960 ± 20
$b\ ^3\Pi_0$	1	(78 202 ± 30)[b]	(~9.6)[c]	Diffuse dbl. head; R − head = 78 327 ± 30
$b\ ^3\Pi_1$	2	80 470 ± 50		Diffuse region.
$C\ ^1\Pi$	0	77 485.3	9.33_3	See Table II.
$C\ ^1\Pi$	1	80 169.3	9.29_6	Diffuse structure; see Table I.
$C\ ^1\Pi$	2	(82 725 ± 15)[b]	(~9.0)[c]	Diffuse dbl. head; R − head = 82 792 ± 20
$C\ ^1\Pi$	3	85 145 ± 60		Diffuse region.
DCl				
$b\ ^3\Pi_2$	0	74 846.9	4.90_5	See Table III.
$b\ ^3\Pi_1$	0	75 133.9	5.10_0	See Table III.
$b\ ^3\Pi_0$	0	75 482.2	5.21_8	See Table III.
$b\ ^3\Pi_1$	1	77 091.0	4.97_1	See Table III.
$b\ ^3\Pi_1$	2	(78 990 ± 15)[b]	(~4.9)[c]	Diffuse dbl. head; R − head = 79 041 ± 20
$D^{35}Cl$				
$C\ ^1\Pi$	0	77 497.6	4.90_9	See Table IV.
$C\ ^1\Pi$	1	79 456.0	4.77_7	See Table IV.
$C\ ^1\Pi$	2	81 348.0	4.65_7	See Table IV.
$C\ ^1\Pi$	3	83 175.8	4.54_1	See Table IV.
$C\ ^1\Pi$	4	84 941.7	4.42_8	See Table IV.
$D^{37}Cl$				
$C\ ^1\Pi$	0	77 497.6	4.90_9	See Table IV.
$C\ ^1\Pi$	1	79 453.0	4.76_7	See Table IV.
$C\ ^1\Pi$	2	81 342.4	4.64_5	See Table IV.
$C\ ^1\Pi$	3	83 167.9	4.52_4	See Table IV.
$C\ ^1\Pi$	4	84 932.0	4.40_9	See Table IV.

[a] As is usual with light molecules, the apparent values of the band origins and rotational constants are somewhat dependent on the numerical methods employed. See text for discussion of the determination of these constants. In all cases $|q| = |B^+ - B^-| \leqq 0.015$ cm^{-1}.

[b] Unresolved Q "head."

[c] Estimated from head separations.

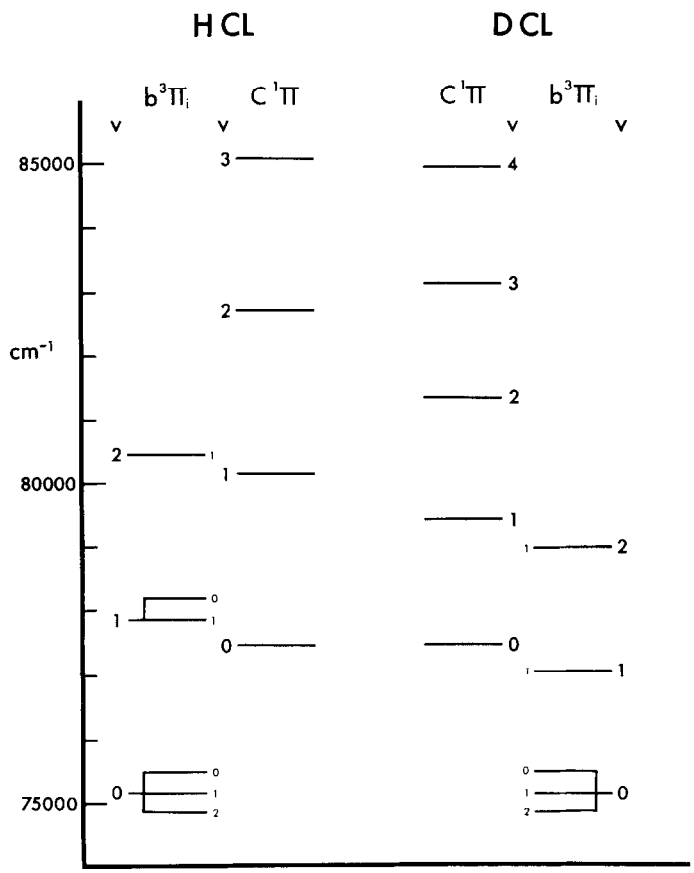

FIG. 3. Observed vibrational structure of the $b\ ^3\Pi_i \leftarrow X\ ^1\Sigma^+$ and $C\ ^1\Pi \leftarrow X\ ^1\Sigma^+$ transitions of HCl and DCl. The Ω values of the appropriate $b\ ^3\Pi_i$ components are indicated as well as the vibrational assignments.

the approximate relation (*16*)

$$R(J) - Q(J) \cong Q(J) - P(J) \cong \Delta_1 F'(J). \tag{1}$$

To determine the band origins and the upper state rotational constants, rotational lines for each Λ-type doubling component were fitted, by the method of least squares, to the equation (*16*)

$$\nu_0 = \nu_{\text{obs}} + B''J''(J''+1) - D''J''^2(J''+1)^2 + H''J''^3(J''+1)^3 - B_v'J'(J'+1) + D_v'J'^2(J'+1)^2, \tag{2}$$

where the appropriate lower state constants were taken from Table VI. This method is equivalent to deriving the rotational constants from the observed upper

TABLE VI

ROTATIONAL CONSTANTS FOR THE $X\ ^1\Sigma^+$ STATE

Species	B_0	$D_0 \times 10^4$	$H_0 \times 10^8$
$H^{35}Cl$	10.44025[a]	5.2835[a]	1.646[a]
$D^{35}Cl$	5.39226[b]	1.4006[b]	
$D^{37}Cl$	5.3757[c]	1.359[c]	

[a] Taken from Ref. (*14*).
[b] Taken from Ref. (*13*).
[c] Taken from Ref. (*15*).

TABLE VII

MOLECULAR CONSTANTS FOR THE $b\ ^3\Pi_i$ AND $C\ ^1\Pi$ STATES OF HCl AND DCl[a]

	T_m[b]	Y_{10} ($\simeq\omega_e$)	Y_{20} ($\simeq -x\omega_e$)	Y_{30} ($\simeq y\omega_e$)	Y_{01} ($\simeq B_e$)	Y_{02} ($\simeq -\alpha_e$)	r_e (Å)
$H^{35}Cl$							
$b\ ^3\Pi_1$	73 712.	2900.	−79.		10.16	−0.6	1.301
$C\ ^1\Pi$	76 092.8	2817.5	−66.0		9.44	−0.15	1.350
$D^{35}Cl$							
$b\ ^3\Pi_1$	74 133.5	2015.4	−29.1		5.153	−0.12	1.311
$C\ ^1\Pi$	76 492.7	2027.1	−34.98	0.39	4.962	−0.120	1.336
$D^{37}Cl$							
$C\ ^1\Pi$	76 494.4	2023.8	−34.79	0.38	4.962	−0.124	1.334

[a] See footnote a, Table V. Unless otherwise indicated, all values are in cm^{-1}.
[b] T_m is the separation between the $v'' = 0$ level of $X\ ^1\Sigma^+$ and the minimum of the potential curve for the upper state.

state term levels. Except for badly blended lines, all data in Tables I–IV were treated in this manner.

For each Λ-type doubling component we initially calculated (a) B_v', D_v', and ν_0, and (b) B_v' and ν_0 with $D_v' = D''$ from Eq. (2). In each case ν_0 remained almost constant, the D_v' determined from the second-order solution did not differ appreciably from D'', and the standard deviations for the second-order solutions were approximately equal to those for the first-order solutions. The B_v values reported in Table V are averages of the values obtained from the first- and second-order solutions for both B_v^+ and B_v^-. In all cases $|q| = |B^+ - B^-| \leqq 0.015\ cm^{-1}$. The maximum deviations from the averages reported in Table V are approximately 0.2–0.3 cm^{-1} for ν_0 and approximately 0.005–0.02 cm^{-1} for B_v. To reproduce accurately any given set of the observed rotational frequencies, a more exact set of constants (to more decimal places) than those listed in Table V is required. Molecular constants were obtained by least squares techniques from the data in

Table V. The minimum number of constants necessary to reproduce the band origins and rotational constants to our experimental uncertainty is included in Table VII.

The Dunham isotope relationships (*16*) were used to confirm the vibrational numbering of the $C^1\Pi$ state of DCl. From the data for $D^{35}Cl$ the shifts in the origins for $D^{37}Cl$ were calculated to be ~0.0, 2.8, 5.4, 7.8, and 10.0 cm^{-1} for the $v' = 0, 1, 2, 3$, and 4 levels, respectively. The corresponding observed shifts (see Table V) are ~0.0, 3.0, 5.6, 7.9, and 9.8 cm^{-1}, all of which are within the estimates of experimental errors.

The $H^{35}Cl$ levels for the $C^1\Pi$ state are observed at lower frequencies (<2% lower) than predicted from the $D^{35}Cl$ data. Just the opposite is true for the $b^3\Pi_1$ state of $H^{35}Cl$; in this case the predicted $H^{35}Cl$ levels are observed at higher frequencies (<2% higher) than predicted from the $D^{35}Cl$ data. These results seem to indicate that small vibrational perturbations exist in both the $C^1\Pi$ and $b^3\Pi_1$ levels of either or both molecules (i.e., in HCl the C levels appear to pushed downward and the b levels appear to be pushed upward and/or in DCl the C levels appear to be pushed upward while the b levels appear to be pushed downward). Figure 3 shows that the relative positions of the vibrational levels of the b and C states in the two molecules are ordered such that a mutual perturbation between $b^3\Pi_1$ and $C^1\Pi$ is most likely partially responsible for the observed shifts (see also Discussion below). In all cases the isotopic relationships correctly predict, within our combined experimental errors for the various molecules, the respective rotational constants.

DISCUSSION

There are several features of these spectra which require further discussion. The first is the assignment of the "B" state to a $^3\Pi_i$ state, designated here as the b state. Such an assignment is immediately suggested by the occurrence, within a 650 cm^{-1} interval, of three isolated bands with $\Delta\Lambda > 0$, one of which has $J = 2$ for its lowest rotational level (see Table III and Fig. 1). A $^3\Pi_i$ (case a) $\leftarrow {}^1\Sigma^+$ transition should exhibit three subbands $^3\Pi_2 - {}^1\Sigma^+$, $^3\Pi_1 - {}^1\Sigma^+$, and $^3\Pi_0 - {}^1\Sigma^+$ which are more or less equally spaced with $\nu_0(^3\Pi_2) - \nu_0(^3\Pi_1) \simeq \nu_0(^3\Pi_1) - \nu_0(^3\Pi_0) \simeq A$. For a case a triplet state of HCl, one would estimate that the splitting constant, A, should be of the order of ½ of the A value for the $X^2\Pi_i$ state of HCl^+, which is (*16*) ½(−643.4) = −322 cm^{-1}. Table V shows that $\nu_0(^3\Pi_2) - \nu_0(^3\Pi_1)$ is −287.4 and −302.6 cm^{-1} for DCl and HCl, respectively, while the corresponding $\nu_0(^3\Pi_1) - \nu_0(^3\Pi_0)$ values are −348.4 and −347.8 cm^{-1}. In addition one can see that the effective B values in Table V for the three components under discussion obey approximately the case a relation (*16*):

$$B^{\text{eff}} \simeq B^t \left(1 \pm \frac{2B^t}{A}\right). \tag{3}$$

Taking $B^t \simeq B(^3\Pi_1)$ and $A = 320$ cm^{-1}, one obtains $B^{\text{eff}}(^3\Pi_2) = 9.26$ and 4.94 cm^{-1} and $B^{\text{eff}}(^3\Pi_0) = 10.48$ and 5.26 cm^{-1} for HCl and DCl, respectively, which are reasonably close to the corresponding observed values. Both this result and the slightly unequal separation of the three subband origins indicate that the central (i.e., $^3\Pi_1$) component is interacting with another $\Omega = 1$ state (e.g., a $^1\Pi_1$ state) lying at higher energy. In such cases, a better estimate of A and B^t in Eq. (3) is obtained from $\frac{1}{2}[\nu_0(^3\Pi_2) - \nu_0(^3\Pi_0)] = A$ and $\frac{1}{2}[B(^3\Pi_2) + B(^3\Pi_0)] = B^t$. From Table V, these values are A(HCl) = 325 cm^{-1}, A(DCl) = 318 cm^{-1}, B^t(HCl) = 9.77 cm^{-1}, and B^t(DCl) = 5.07 cm^{-1}, which when substituted into Eq. (3) yield: (a) for HCl, $B^{\text{eff}}(^3\Pi_2) = 9.17$ cm^{-1} and $B^{\text{eff}}(^3\Pi_0) = 10.37$ cm^{-1} and (b) for DCl, $B^{\text{eff}}(^3\Pi_2) = 4.91$ cm^{-1} and $B^{\text{eff}}(^3\Pi_0) = 5.23$ cm^{-1}. The excellent agreement of these results with the effective rotational constants in Table V, the agreement of the resulting A values with estimates from $X^2\Pi_i$ of HCl^+, together with the occurrence of an $\Omega = 2$ state (i.e., $^3\Pi_2$ or a Δ-type) as the lowest energy component, essentially requires the assignment of the bands under discussion to a $^3\Pi_i \leftarrow {}^1\Sigma^+$ transition.

The preceding discussion in turn strongly implies that the configuration associated with the $b^3\Pi_i$ state is $\pi^3\sigma$, and that there should be a $^1\Pi$ state within a few thousand cm^{-1} to higher energy which is associated with the same configuration. The only observed Π-type state within 6500 cm^{-1} above $b^3\Pi_i$ is $C^1\Pi$, which lies $\sim$2350 cm^{-1} above the b state. Assuming the b and C states to be the $^3\Pi_i$ and $^1\Pi$ states from a $\pi^3\sigma$ configuration, one can treat their interactions using expressions appearing in the literature (*8a*). Assuming 2388 cm^{-1} as the separation[3] of $C^1\Pi$ from the $b^3\Pi_i$ state and $A = 325$ cm^{-1}, one can estimate that the perturbed (i.e., observable) separation of $C^1\Pi$ and $b^3\Pi_1$ should be 2364 cm^{-1}, while the relative intensities of the $C - X$ to $b - X$ transitions should be of the order of 56. These values compare favorably with the observed values of 2343 cm^{-1} and 40 to 50 for these quantities (see Table V and the preceding section). The fact that the $b^3\Pi_2 \leftarrow X^1\Pi^+$ and $b^3\Pi_0 \leftarrow X^1\Sigma^+$ subbands are of comparable intensity (see preceding section) suggest that these subbands become allowed by rotational mixing, principally with the $b^3\Pi_1$ state, and that there are no $^1\Sigma^+$ states in the region which couple effectively with the $^3\Pi_0{}^+$ component. The observed intensity distribution for the $b^3\Pi_i$ subbands taken together with the observation that there is no detectable difference between the band origins for $b^3\Pi_0{}^+ \leftarrow X^1\Sigma^+$ and $b^3\Pi_0{}^- \leftarrow X^1\Sigma^+$ indicates that case c effects and/or interactions with states from other configurations must be relative minor for the $b^3\Pi_i$ state. The net result of all the above considerations are that the "B" state is very nearly a case a $^3\Pi_i$ state which is interacting *principally* with the $C^1\Pi$ state and that both states originate from the same $\pi^3\sigma$ configuration. However, the diffuseness of many of the observed bands (see

[3] If the C $^1\Pi$ state is shifted up by approximately the same amount that the b $^3\Pi_1$ state is shifted below the multiplet "center," the approximate singlet–triplet separation would be 2388 cm^{-1}.

Tables I–V) indicates that the $b^3\Pi_i$ and/or $C^1\Pi$ states also interact with one or more of the continuum states $A^1\Pi$, $a^3\Pi_i$, or $t^3\Sigma^+$.

ACKNOWLEDGMENTS

The authors wish to thank R. H. Naber for his assistance in photographing these spectra and Dr. M. Krauss for several helpful discussions.

RECEIVED: August 18, 1969

REFERENCES

1. P. CONNES, J. CONNES, W. S. BENEDICT, AND L. D. KAPLAN, *Astrophys. J.* **47**, 1230 (1967).
2. J. ROMAND, *Ann. Phys. (Paris)* **4**, 527 (1949).
3. J. K. JACQUES AND R. F. BARROW, *Proc. Phys. Soc. (London)* **73**, 538 (1959).
4. (a) W. C. PRICE, *Proc. Roy. Soc. Ser. A* **167**, 216 (1938); (b) S. G. TILFORD AND M. L. GINTER, unpublished data; (c) M. G. WAGGONER AND A. L. SMITH, private communication.
5. R. S. MULLIKEN, *Phys. Rev.* **61**, 277 (1942), and references therein.
6. J. G. STAMPER, *Can. J. Phys.* **40**, 1274 (1962).
7. R. K. NESBET, *J. Chem. Phys.* **41**, 100 (1964).
8. (a) R. S. MULLIKEN, *Phys. Rev.* **57**, 500 (1940); (b) **51**, 310 (1937); (c) **50**, 1017 (1936).
9. P. G. WILKINSON AND E. T. BYRAM, *Appl. Opt.* **5**, 581 (1965).
10. H. M. CROSSWHITE, private communication.
11. L. E. GIDDINGS, private communication.
12. J. T. VANDERSLICE, S. G. TILFORD, AND P. G. WILKINSON, *Astrophys. J.* **141**, 395 (1965).
13. D. H. RANK, B. S. RAO, AND T. A. WIGGINS, *J. Mol. Spectrosc.* **17**, 122 (1965).
14. D. H. RANK, D. P. EASTMAN, B. S. RAO, AND T. A. WIGGINS, *J. Opt. Soc. Amer.* **52**, 1 (1962).
15. D. U. WEBB AND K. NARAHARI RAO, *J. Mol. Spectrosc.* **28**, 121 (1968).
16. G. HERZBERG, "Molecular Spectra and Molecular Structure. I. Spectra of Diatomic Molecules," 2nd. ed. Van Nostrand, Princeton, New Jersey. 1950.